

# Appendix 1

## Assessing the impact of non-pharmaceutical interventions on SARS-CoV-2 transmission in Switzerland

Joseph. C. Lemaitre<sup>1,\*</sup>, Javier Perez-Saez<sup>2,\*</sup>, Andrew S. Azman<sup>2</sup>, Andrea Rinaldo<sup>1,3</sup>, and Jacques Fellay<sup>4,5</sup>

<sup>1</sup>Laboratory of Ecohydrology, School of Architecture, Civil and Environmental Engineering, École Polytechnique Fédérale de Lausanne, CH-1015 Lausanne

<sup>2</sup>Department of Epidemiology, Johns Hopkins Bloomberg School of Public Health, Baltimore, Maryland, USA

<sup>3</sup>Dipartimento di Ingegneria Civile Edile ed Ambientale, Università di Padova, I-35131 Padua, Italy

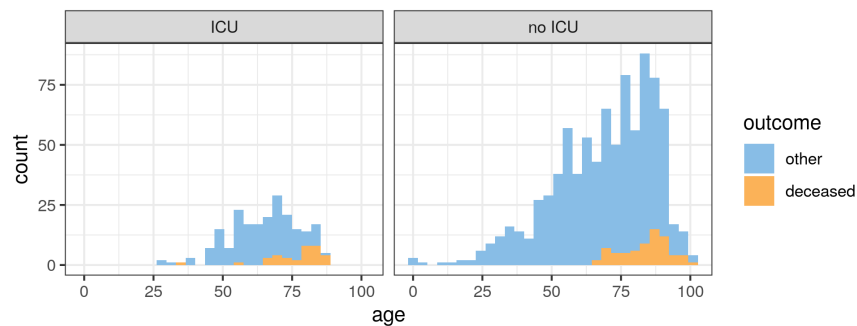
<sup>4</sup>School of Life Sciences, École Polytechnique Fédérale de Lausanne, CH-1015 Lausanne

<sup>5</sup>Precision Medicine Unit, Lausanne University Hospital and University of Lausanne, CH-1011 Lausanne

\*Share first authorship

### 1 Canton of Vaud hospitalization data

We had access to individual-level data from 1093 patients hospitalized in the canton of Vaud up to April 14, 2020. Of all patients, 41% (448/1093) were female and 59% were male (645/1093) with a median age of 70 years (Supplementary Material, SM, Figure 1). Of all the hospitalized cases, 20% (214/1093) required use of an Intensive Care Unit (ICU).

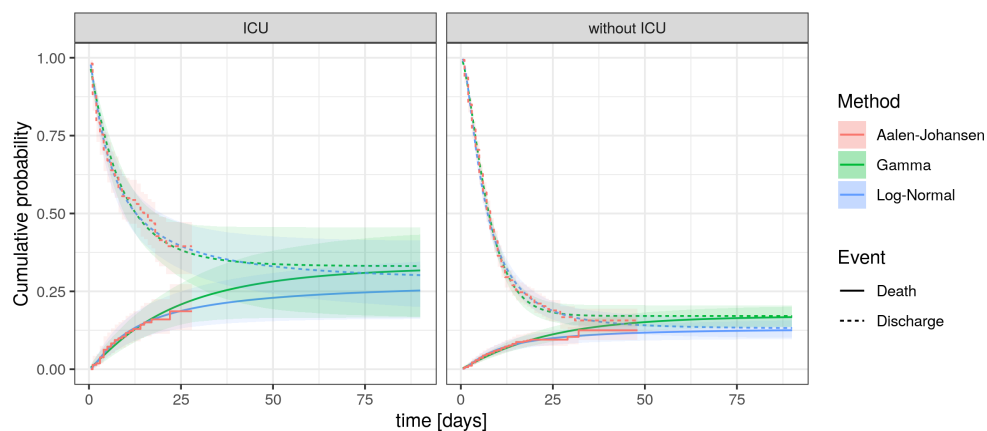


SM Figure 1: Age distribution of patients hospitalized for COVID-19 in the canton of Vaud up to April 14. Hospitalized individuals are divided in two subgroups depending on if they were treated in ICU (left) or not (right) during their stay. Moreover, only the 777 patients with known outcome are displayed here. We highlight the outcome: either death (orange) or discharge/transfer to another hospital (blue).

Of 777 patients with a known outcome on April 14, 104 died (13%). We estimate the hospitalized Case Fatality Ratio (hCFR) by adjusting for the distribution of time hospitalization to death accounting for the fact that outcomes have not been yet observed for all patients (right-censoring). To account for multiple outcomes (death and discharge), we implement a parametric competing risk survival model similar to that of [6]. We follow a Bayesian approach proposed in [1] that enables us to fit parametric distributions to times to events using accelerated failure models. This method allows for the joint estimation of the probability of each event type and the distributions of times to events. In this case we are interested in the probability of death, i.e. the hCFR. A COVID-19 modeling study in France identified mixtures of probabilities of times to death, with a group dying faster with exponentially-distributed times and one dying slower [16]. We

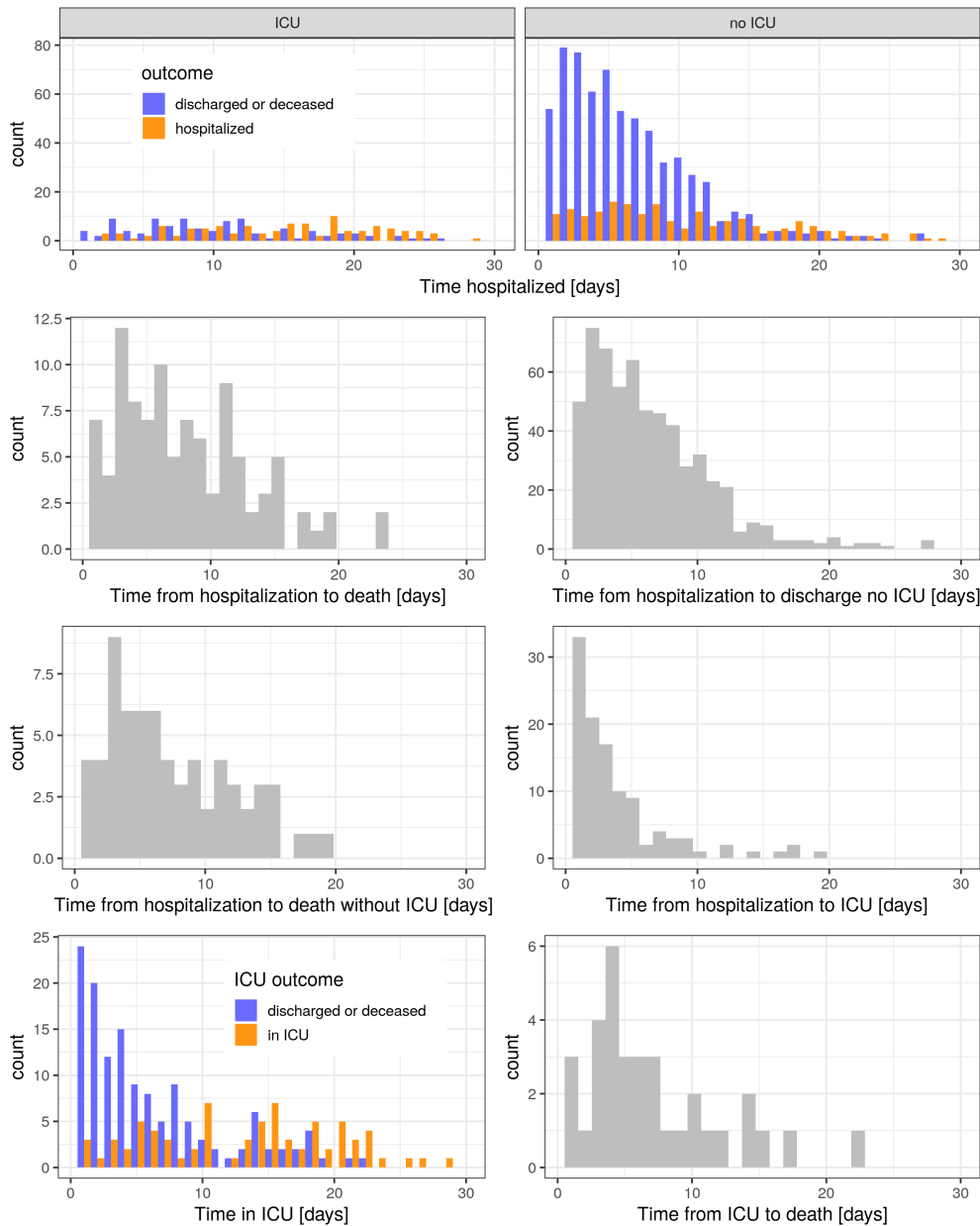
therefore extend the Bayesian survival framework to test for mixture in times to death and recovery. We did not take into model patients being discharged from ICU and subsequently dying which was the case for 4/138 patients with known outcome. We neither accounted for multiple ICU stays per patient since we did not have that information. We fit both Gamma and Log-Normal distributions separately to patients that did not go into ICU, and patients that did. For the former, we model times from hospitalization to death or discharge, and for the latter times from ICU entry to both outcomes. Models were fit with Stan [4], and selection was done using Bayesian leave-one-out cross-validation [21].

Times to death and discharge were best described by log-normal distributions with a single group both for patients having required ICU or not (SM Fig. 2). When accounting for right-censoring and assuming log-normally distributed times to events, we estimate an overall hCFR of 16.0% (95% credible interval, CrI: 12.5-19.8), resulting from a hCFR of 28.1% (95% CrI: 16.4-40.9) for patients requiring ICU and 13.0% (95% CrI: 9.9-16.6) for patients that did no require it. Estimated hCFRs were slightly higher when assuming gamma-distributed times to events (overall hCFR of 20.3%, 95% CrI: 15.9-24.1).



SM Figure 2: Survival functions of death and discharge for hospitalized patients and patients in ICU. The lines represent the mean estimated cumulative probability of dying (full) and 1 minus the cumulative probability of discharge (dotted) estimated with non-parametric (Aalen-Johansen estimator, shading gives the 95% CI) and parametric (assuming gamma and log-normal distributions, shading indicate the 95% CrI) methods. Time is in days from hospitalization for patients that did not require ICU, and time from ICU admission for those that did. The point at which the lines join represents the probability that the final outcome is death, which was estimated to be 28.1% (95% CrI: 16.4-40.9) for patients in ICU and 13.0% (95% CrI: 9.9-16.6) for patients not requiring ICU based on the log-normal distribution.

The distribution of times of hospitalization processes are shown in SM Fig. 3, and fitted distribution parameters given in SM Table 1.



SM Figure 3: Data from canton de Vaud showing times to key hospitalization events. In order to perform this analysis, we split patients in two categories: those who did not go through ICU during their stay and those who did. From left to right, top to bottom: total length of hospital stay for patients that went to ICU, then similarly for patient that did not. Then we show the time to death for all patients, followed by both the time to discharge and to death for non-ICU patients. The last three graphs concerns ICU patients and detail ICU focused estimate: time from hospitalization to ICU, time in ICU and time from ICU to death. When meaningful, we show both currently hospitalized patient (orange) and already out-of-hospital patients (blue).

SM Table 1: Observed hospitalization time distributions. All times are in days and taken from the date of hospitalization if not specified otherwise. Note that these estimates are biased due to right-censoring of observations and probably under-estimate the true distributions. SM Table 2 shows estimates that account for right-censoring.

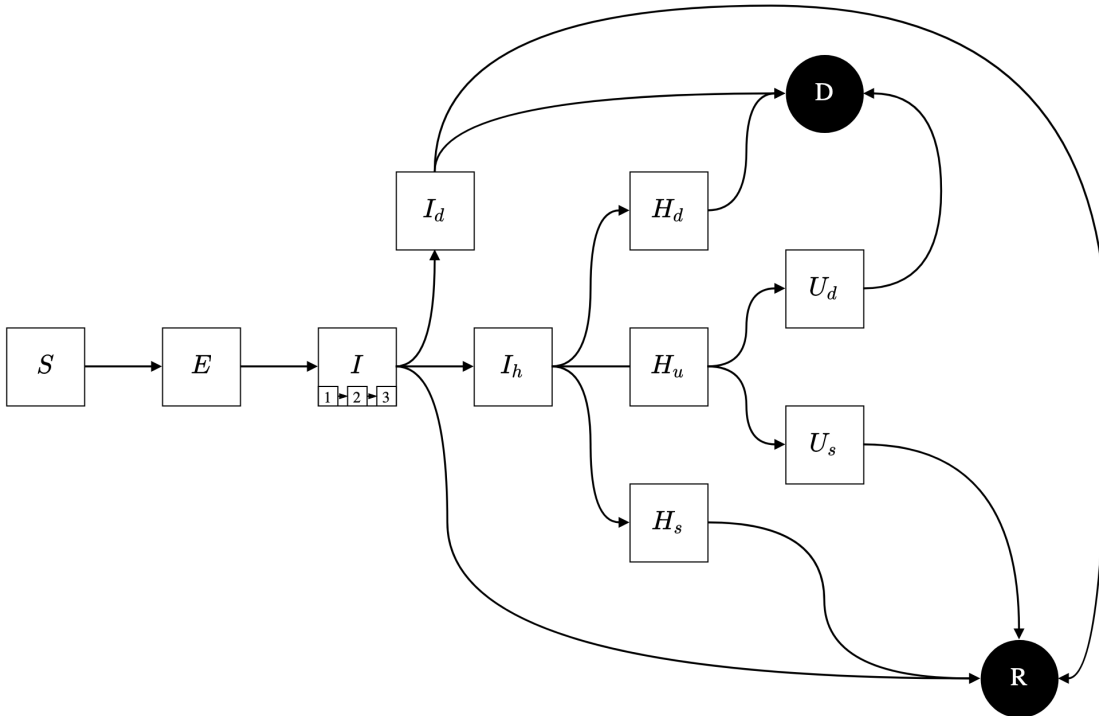
	mean	sd	mean (logscale)	sd (logscale)
Time hospitalized	8.49	6.58	1.81	0.87
Time to death	8.23	6.09	1.80	0.87
Time to discharge without ICU	6.29	4.66	1.56	0.80
Time hospitalized without ICU	7.35	5.79	1.68	0.85
Time to death without ICU	7.84	6.27	1.73	0.88
Time to ICU	2.35	3.79	0.18	1.05
Time hospitalized with ICU	13.14	7.50	2.37	0.72
Time in ICU	8.36	6.76	1.69	1.04
Time from ICU to discharge	8.68	6.99	1.71	1.07
Time from ICU to death	6.97	4.98	1.68	0.77

SM Table 2: Estimated parameters of hospitalization time distributions. These estimates differ from observed values given in Table 1 by accounting for right-censoring of observations. We report time from hospitalization to discharge or death, and from ICU admission to discharge or death. Estimates were obtained using competing risk survival model as described in section 1. Parameters are given in terms of their posterior mean and 95% CrI (in parenthesis). For the log-normal distribution the parameters correspond to the mean and SD of the logarithm of the distribution.

Group	Event	Log-Normal			Gamma	
		median	mean-log	SD-log	scale	shape
Without ICU	Death	10 (7.3-16)	2.3 (2-2.8)	1.2 (0.95-1.5)	21 (21-22)	1.1 (0.83-1.4)
	Discharge	6.1 (5.6-6.6)	1.8 (1.7-1.9)	0.93 (0.87-0.99)	4.3 (4.4-4.2)	1.8 (1.6-2)
ICU	Death	13 (6.2-30)	2.6 (1.8-3.4)	1.3 (0.87-1.9)	21 (12-23)	1.2 (0.74-1.9)
	Discharge	6.4 (4.3-9.3)	1.8 (1.5-2.2)	1.3 (1.1-1.6)	9.1 (8.1-11)	1 (0.75-1.4)

## 2 Model Description

We build a COVID-19 compartmental transmission model based on the Susceptible Exposed Infected Recovered (SEIR) template with three I compartments. The schematic with the different transitions and compartments is shown in SM Fig. 4. Infected individuals have some probability of developing severe symptoms which require hospitalization after a delay from symptom onset ( $I_h$ ). Hospitalization can lead to recovery or death, either through normal hospitalization ( $H_s$  and  $H_d$  respectively) or passing through Intensive Care Units (ICUs) ( $U_s$  and  $U_d$  respectively). Data from the canton of Vaud show a high proportion of deaths outside of hospitals ( $\approx 50\%$ ), we therefore also include a pathway from infection to death without passing through hospitalization ( $I_d$ ).



SM Figure 4: Schematic diagram of COVID-19 transmission and hospitalization processes. There are two sinks: Death  $D$  and recovered  $R$ . Each stage with regard to the disease may be implemented with several compartments (subscript numbered boxes) to better represent the time distribution spent in that stage. The model is implemented as a Hidden Markov Model using the POMP package in R [10]. The mean length of stay in compartment  $X$  is determined by the rate parameter  $r_X$  in SM Table 3 and the branching probabilities from  $X$  to  $Y$  are shown in SM Table 4.

The time spent in the observable hospitalization states were used to define the number of stages in each compartment by fitting Erlang distributions to the data of canton de Vaud. To account for right-censoring we do not fit directly to observed times to events but rather to the estimated log-normal distributions described in the survival analysis section above. We fit the rate parameter of the Erlang distributions for shape parameters between 1 and 10 by minimizing the Kullback-Leibler (KL) divergence between the Erlang and estimated log-normal distributions. The final fit was taken to be the one with the smallest KL-divergence.

We found that all hospitalization processes were best represented with exponential distributions (Erlang with shape parameter of 1). Rates of transitions are shown Table 3 and branching probabilities in Table 4.

## 2.1 Model equations

We implemented the model as a discrete-state model based on a Partially-Observed Markov Process (POMP), or equivalently a Hidden Markov Model (HMM), simulating the transitions between compartments as discrete events using stochastic count processes [11, 3]. Let  $N_{AB}(t)$  be the number of individuals transiting between compartments  $A, B \in \mathcal{X}$  in the time interval  $[0, t)$  where  $\mathcal{X}$  is the state vector,

$$\mathcal{X} = \{S, E, I_{1,2,3}, I_d, I_h, H_s, H_d, H_u, U_s, U_d, R, D\}$$

The number of transitions during a time-step  $\Delta t$  is  $\Delta N_{AB}(t) = N_{AB}(t + \Delta t) - N_{AB}(t)$ . We model time-varying  $R_0(t) = \beta(t)/(3r_I)$  as a geometric random walk defined by its calibrated variance, where  $\beta$  is the transmission parameter and  $1/(3r_I)$  is the mean duration spent in the infectious compartments  $I_1$  to  $I_3$ . The force of infection is expressed in terms of  $\beta(t)$  in the model. Given the state of the system at time  $t$ ,  $\mathcal{X}_t$ , the model reads:

$$\begin{aligned} \mathbb{P}[\Delta N_{SE}(t) = 1 | \mathcal{X}_t] &= \beta(t) \frac{I_1(t) + I_2(t) + I_3(t)}{P} S(t) \Delta t + o(\Delta t) \\ \mathbb{P}[\Delta N_{EI_1}(t) = 1 | \mathcal{X}_t] &= r_E E(t) \Delta t + o(\Delta t) \\ \mathbb{P}[\Delta N_{I_1 I_2}(t) = 1 | \mathcal{X}_t] &= 3r_I I_1(t) \Delta t + o(\Delta t) \\ \mathbb{P}[\Delta N_{I_2 I_3}(t) = 1 | \mathcal{X}_t] &= 3r_I I_2(t) \Delta t + o(\Delta t) \\ \mathbb{P}[\Delta N_{I_3 I_d}(t) = 1 | \mathcal{X}_t] &= p_{I_d|I_3} \cdot 3r_I I_3(t) \Delta t + o(\Delta t) \\ \mathbb{P}[\Delta N_{I_3 I_h}(t) = 1 | \mathcal{X}_t] &= p_{I_h|I_3} \cdot 3r_I I_3(t) \Delta t + o(\Delta t) \\ \mathbb{P}[\Delta N_{I_3 R}(t) = 1 | \mathcal{X}_t] &= p_{R|I_3} \cdot 3r_I I_3(t) \Delta t + o(\Delta t) \\ \mathbb{P}[\Delta N_{I_d R}(t) = 1 | \mathcal{X}_t] &= p_{R|I_d} \cdot r_I I_d(t) \Delta t + o(\Delta t) \\ \mathbb{P}[\Delta N_{I_d D}(t) = 1 | \mathcal{X}_t] &= p_{D|I_d} \cdot r_I I_d(t) \Delta t + o(\Delta t) \\ \mathbb{P}[\Delta N_{I_h H_d}(t) = 1 | \mathcal{X}_t] &= p_{H_d|I_h} \cdot r_{I_h} I_h(t) \Delta t + o(\Delta t) \\ \mathbb{P}[\Delta N_{I_h H_u}(t) = 1 | \mathcal{X}_t] &= p_{H_u|I_h} \cdot r_{I_h} I_h(t) \Delta t + o(\Delta t) \\ \mathbb{P}[\Delta N_{I_h H_s}(t) = 1 | \mathcal{X}_t] &= p_{H_s|I_h} \cdot r_{I_h} I_h(t) \Delta t + o(\Delta t) \\ \mathbb{P}[\Delta N_{H_s R}(t) = 1 | \mathcal{X}_t] &= r_{H_s} H_s(t) \Delta t + o(\Delta t) \\ \mathbb{P}[\Delta N_{H_u U_d}(t) = 1 | \mathcal{X}_t] &= p_{U_d|H_u} \cdot r_{H_u} H_u(t) \Delta t + o(\Delta t) \\ \mathbb{P}[\Delta N_{H_u U_s}(t) = 1 | \mathcal{X}_t] &= p_{U_s|H_u} \cdot r_{H_u} H_u(t) \Delta t + o(\Delta t) \\ \mathbb{P}[\Delta N_{H_d D}(t) = 1 | \mathcal{X}_t] &= r_{H_d} H_d(t) \Delta t + o(\Delta t) \\ \mathbb{P}[\Delta N_{U_s R}(t) = 1 | \mathcal{X}_t] &= r_{U_s} U_s(t) \Delta t + o(\Delta t) \\ \mathbb{P}[\Delta N_{U_d D}(t) = 1 | \mathcal{X}_t] &= r_{U_d} U_d(t) \Delta t + o(\Delta t) \end{aligned} \tag{1}$$

assuming that  $\mathbb{P}[\Delta N_{XY} > 1 | \mathcal{X}_t] = o(\Delta t) \forall X, Y \in \mathcal{X}$ . Branching probabilities from stage  $X$  to  $Y$  are noted  $p_{Y|X}$  and rates of stay in stage  $X$  is noted  $r_X$ . The ensuing stochastic variations of the state variables are:

$$\begin{aligned}
\Delta E(t) &= \Delta N_{SE}(t) - \Delta N_{EI_1}(t) \\
\Delta I_1(t) &= \Delta N_{EI_1}(t) - \Delta N_{I_1I_2} \\
\Delta I_2(t) &= \Delta N_{I_1I_2} - \Delta N_{I_2I_3} \\
\Delta I_3(t) &= \Delta N_{I_2I_3} - \Delta N_{I_3I_d} - \Delta N_{I_3I_h} - \Delta N_{I_3R} \\
\Delta I_d(t) &= \Delta N_{I_3I_d} - \Delta N_{I^dR} - \Delta N_{I^dD} \\
\Delta I_h(t) &= \Delta N_{I_3I_h} - \Delta N_{I_hH_d} - \Delta N_{I_hH_u} - \Delta N_{I_hH_s} \\
\Delta H_s(t) &= \Delta N_{I_hH_s} - \Delta N_{H_sR} \\
\Delta H_d(t) &= \Delta N_{H_dH_u} - \Delta N_{H_dD} \\
\Delta H_u(t) &= \Delta N_{I_hH_u} - \Delta N_{H_uU_d} - \Delta N_{H_uU_a} - \Delta N_{H_uU} \\
\Delta U(t) &= \Delta N_{H_uU} - \Delta N_{UR} \\
\Delta U_d(t) &= \Delta N_{H_uU_d} - \Delta N_{U_dD} \\
\Delta D(t) &= \Delta N_{I^dD} + \Delta N_{U_dD} + \Delta N_{H_dD} \\
\Delta R(t) &= \Delta N_{I_3R} + \Delta N_{I^dR} + \Delta N_{H_sR} + \Delta N_{UR} \\
S(t) &= P - \sum_{X \in \mathcal{X} \setminus \{S\}} X(t),
\end{aligned} \tag{2}$$

where the equation for  $S(t)$  enforces a constant total population. The total population for each canton and for Switzerland is taken from the 2018 estimate of the Federal Statistical Office [19].

SM Table 3: Transition rates from each compartment of the model. Compartments  $I_{1,2,3}$  are composed of several stages so the rate of exit from each one is  $3r_I$ . We parameterize the model conditioning on a mean generation time of 5.2 days [5], and an exposed and non-infectious duration of 2.9 days [7], yielding a mean duration of 4.6 days in the infectious compartments. All rates are given in  $\text{day}^{-1}$  and the subscript subscript in the parameter names indicate the compartment from which exits happen at the given rate.

Rate	Source	Value or starting bound	Corresponding duration
$r_E$	[7]	1/2.9	infected but non-infectious state
$r_I$	[7, 5]	1/4.6	infectious state
$r_{I_h}$	[17]	1/1.6	end of the infectious period to hospitalization
$r_{H_s}$	Vaud data	1/7.6	hospitalization to discharge
$r_{H_d}$	Vaud data	1/23.7	hospitalization to death
$r_{H_u}$	Vaud data	1/2.35	hospitalization to ICU admission
$r_{U_s}$	Vaud data	1/9.3	ICU admission to discharge
$r_{U_d}$	Vaud data	1/25.6	ICU admission to death
$r_{I_d}$	Fitted	1/50 – 1/1	end of the infectious period to death when not hospitalized

SM Table 4: Branching probabilities of the model. The probability from stage  $A$  to stage  $B$  is  $p_{B|A}$ . There are seven different pathways from susceptible to either death or recovery. We assume that the proportion of severe infections that have severe symptoms which would require hospitalization is of 7.5% [22], that 50% of deaths happen outside of hospitals (data from cantons of Vaud as above and Geneva from OpenZH), that the hospitalized case fatality ratio is of 16% (data from canton of Vaud, see above), the probability of going into ICU for hospitalized patients is of 20% (data from canton of Vaud), and an population-level infection fatality ratio (IFR) of 0.75 % which is in the range of published estimates [22, 15].

Parameter	Source	Value	Description
IFR	Assumed	0.0075	Infection fatality ratio
$p_s$	Assumed	0.075	Probability of severe symptoms
$p_h$	Vaud data   IFR	0.31	Probability of hospitalization given severe symptoms
$p_{I_d I_3}$	Vaud data   IFR, $p_s$	$p_s(1 - p_h)$	Probability of death outside of the hospital given severe symptoms
$p_{I_h I_3}$	Vaud data   IFR, $p_s$	$p_s p_h$	Probability of hospitalization given infection
$p_{R I_3}$	Deduced   $p_s$	$(1 - p_s)$	Probability of not having severe symptoms
$p_{D I_d}$	Vaud data   IFR, $p_s$	0.073	Probability of death given severe symptoms and not hospitalized
$p_{R I_d}$	Vaud data   IFR, $p_s$	$1 - p_{D I_d}$	Probability of recovery given severe symptoms
$p_{H_s I_h}$	Vaud data	0.72	probability of discharge without ICU given hospitalization
$p_{H_d I_h}$	Vaud data	0.11	Probability of death given not going into ICU
$p_{H_u I_h, I_s}$	Vaud data	0.61	Probability of ICU given not discharged without ICU
$p_{U_d H_u}$	Vaud data	0.28	Probability of death given ICU

### 3 Model Selection and Fitting/Calibration

We calibrate the model separately for each canton on the daily death and hospitalization until April 24. The calibration procedure is based on a frequentist multiple iterated filtering algorithm (MIF2 [9]). The observation model is formulated as follows:

$$\begin{aligned}
 deaths(t) &\sim Poisson(\Delta D(t)) \\
 \Delta hosp(t) &\sim Skellam(\Delta H(t), \Delta D_H(t) + \Delta R_H(t))
 \end{aligned}$$

where,  $\Delta D(t)$ ,  $\Delta H(t)$ ,  $\Delta D_H(t)$ ,  $\Delta R_H(t)$  are respectively the number of new deaths, hospitalized, and deaths and discharged from hospitals at time  $t$ , and  $\Delta hosp(t)$  is the difference between the number of current hospitalizations at times  $t$  and  $t - 1$ , for which we choose a Skellam distribution [18]. The full log-likelihood of the observation model was taken as the sum of the individual log-likelihoods of the  $\Delta hosp(t)$  and of the  $deaths(t)$ . We did not use cases due to the difference in testing procedure in time and between cantons.

### 4 Assessment of Model Fit

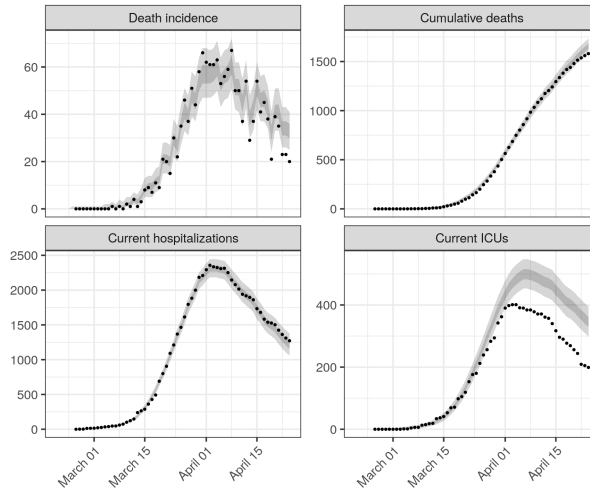
SM Figures 5 and 6 show model fits at the national and cantonal levels respectively. We note that hospitalization processes in all cantons and the national level were parameterized with data from the canton of Vaud. Difference in hospital protocols and procedures in each canton as well as transfers of patient between cantons will cause differences between observed and modelled ICU occupancy.

SM Table 5: Estimated values of  $R_0$  at the beginning of the epidemic (March 01-March 10) and after the implementation of non-pharmaceutical interventions (March 29-April 5). Estimates given in terms of the median and 95% quantile range (in parenthesis).

	March 01-March 10		March 29-April 05	
	median	95% QR	median	95% QR
Switzerland	2.8	(2.5-3.1)	0.4	(0.27-0.6)
Bern	2.4	(2-3)	0.5	(0.26-0.9)
Basel-Landschaft	2.8	(2.2-3.7)	0.22	(0.03-0.7)
Basel-Stadt	3.1	(2.6-3.8)	0.3	(0.13-0.6)
Fribourg	2.7	(2.2-3.4)	0.4	(0.2-0.8)
Geneve	2.6	(2.1-3)	0.5	(0.24-0.8)
Jura	1.4	(1.2-1.6)	0.7	(0.4-1)
Neuchatel	2	(1.7-2.3)	0.6	(0.4-1)
Ticino	4	(3-5)	0.5	(0.29-1)
Vaud	2.7	(2.4-3)	0.5	(0.3-0.8)
Valais	1.8	(1.4-2.2)	0.29	(0.07-0.7)
Zurich	2.3	(1.8-2.8)	0.5	(0.25-0.9)

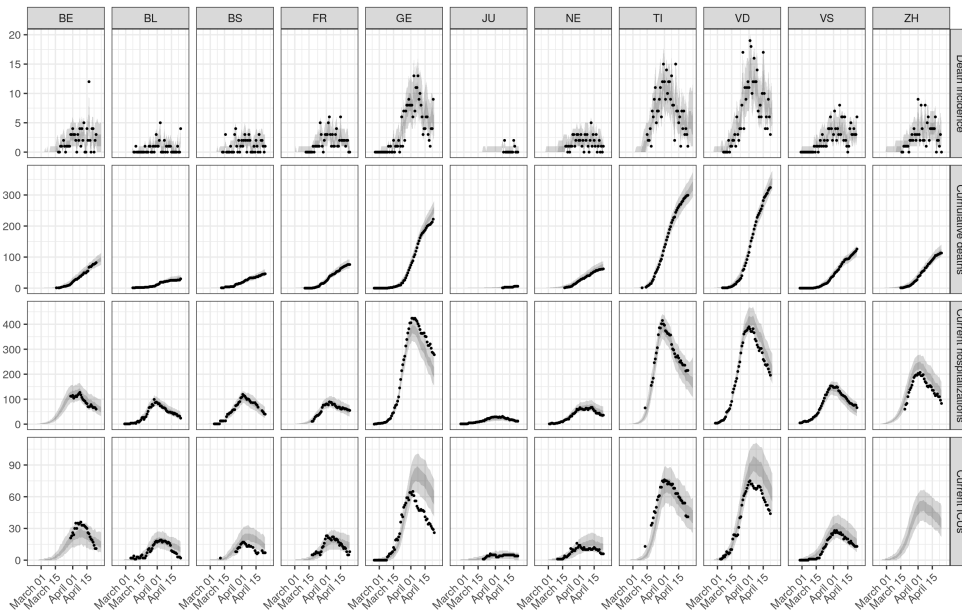
SM Table 6: Estimated proportion of population infected with SARS-CoV-2 as of April 24 2020. Estimates given in terms of the median and 95% quantile range (in parenthesis).

Canton	Proportion infected [%]
Switzerland	3.9 (3.6-4.3)
Bern	1.9 (1.4- 2.6)
Basel-Landschaft	3.9 (2.9-5.0)
Basel-Stadt	6.7 (5.0-8.6)
Fribourg	4.0 (3.0-5.4)
Geneve	11.0 (9.3-13.3)
Jura	4.2 (2.8- 6.5)
Neuchatel	6.7 (4.9-9.1)
Ticino	16.0 (13.5-21.2)
Vaud	8.0 (6.8- 9.3)
Valais	5.5 (4.4-7.4)
Zurich	2.3 (1.8- 2.9)

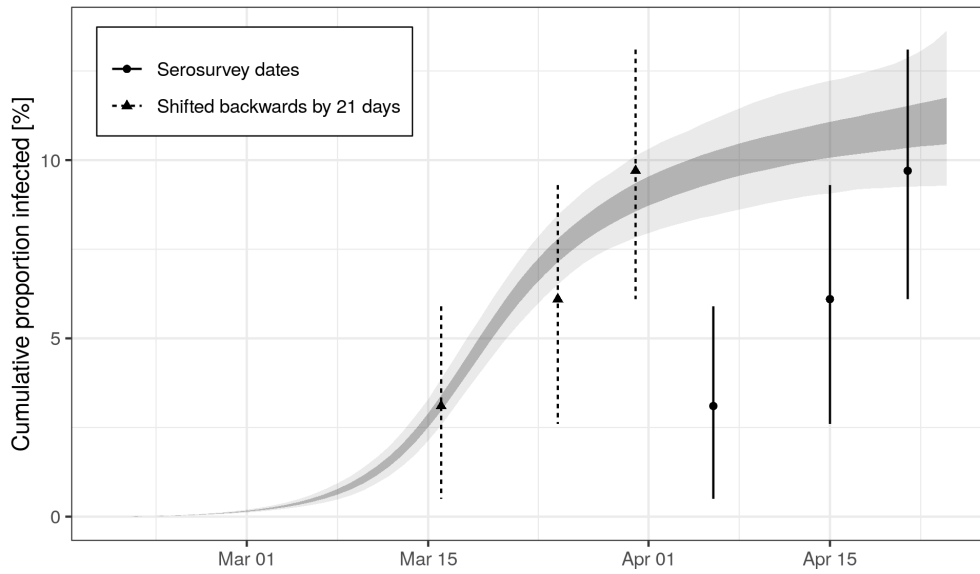


SM Figure 5: Model fit at national level. Model results are given in terms of the 95% (light gray) and 50% quantile ranges of the smoothing distribution of  $R_0$  at the maximum likelihood estimates of inferred parameters. Data (points) from [14]

. Our model tends to overestimate current ICU using time distributions from canton de Vaud, while death (cumulative and incidence) and current hospitalization are well captured. We do not model cases reporting due to differences in the reporting processes in time.



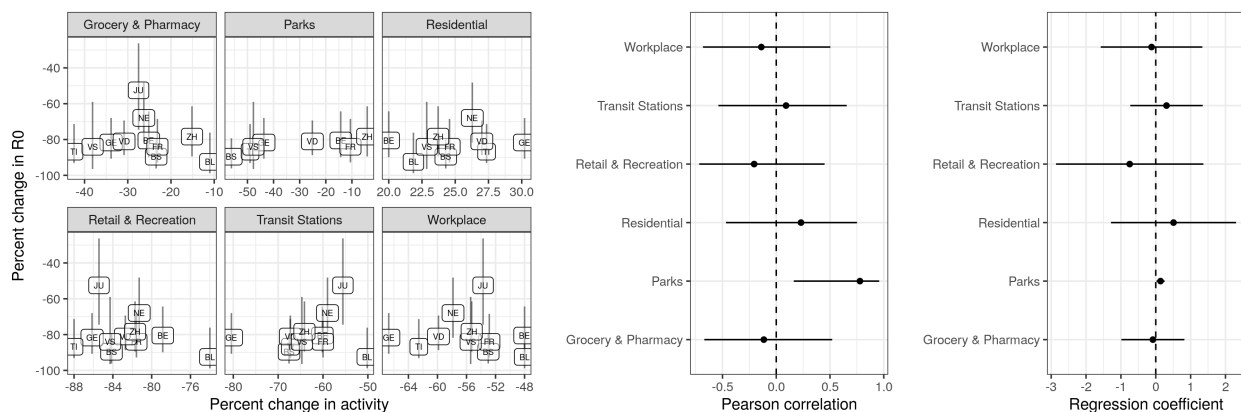
SM Figure 6: Cantonal level fits, with the same legend as in SM Fig. 5. Data (points) from [13].



SM Figure 7: Qualitative comparison between modelled proportion of people infected in the canton of Genève and seroprevalence estimates. Model estimates (ribbons, dark shading give the IQR and light shading the 95% quantile range) are compared to seroprevalence estimates (points, error bars give the 95% CrI) taken from Figure 1 in [20] [Accessed May 15 2020]. Seroprevalence estimates do not correspond to infection status on the date of the survey due to the delay between infection and seroconversion. We roughly account for this delay by plotting seroprevalence estimates shifted backwards in time to represent the delay between infection and symptom onset (6 days [2]) and from symptom onset to seroconversion (about 80% of seroconversions occur within 15 days [8]), resulting in a total shift of 21 days. Note that seroprevalence estimates were not used in model fitting. Quantitative evaluation of adequacy between modelled proportion infected and seroprevalence estimates would require modelling explicitly seroconversion.

## 5 Mobility analysis

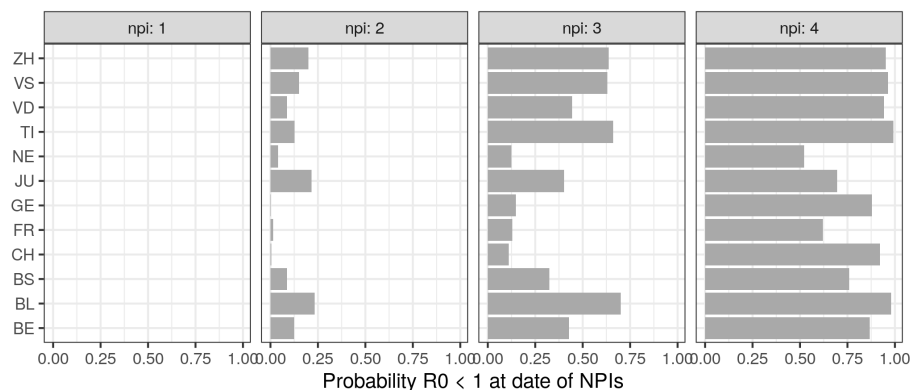
SM Fig. 8 shows the cross-cantonal correlation between reduction in  $R_0$  and mobility changes.



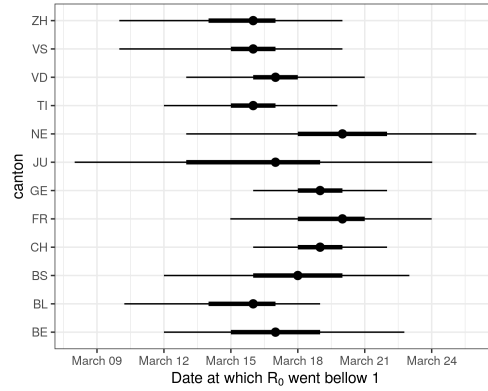
SM Figure 8: Cross-cantonal association between reductions in  $R_0$  and activity-related mobility. Left: Scatter plots of maximal reduction in activity against maximal estimated reduction in  $R_0$ , vertical error bars indicate the 95% quantile range of  $R_0$ . Center: correlation coefficients per activity. Left: Regression coefficient per activity. A regression coefficient of 1 means that a 1% decrease in activity was associated with a 1% decrease in  $R_0$ .

## 6 Changepoint analysis

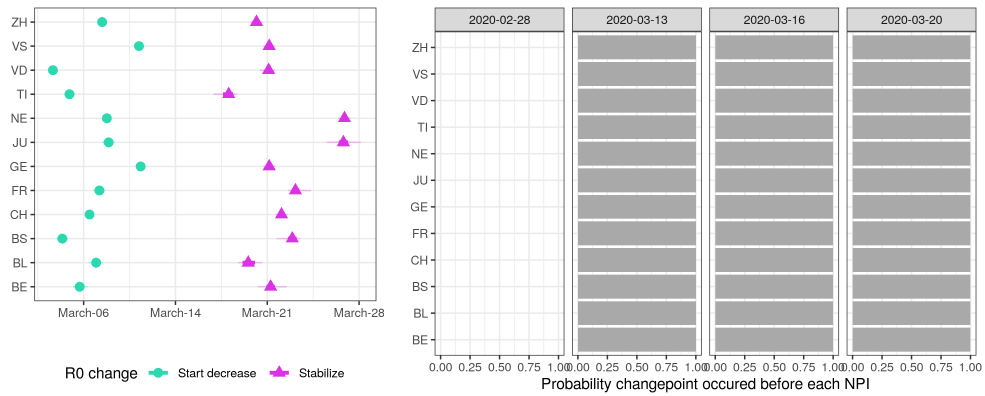
We used Bayesian changepoint models to infer dates of changes in  $R_0$  reduction using the *mcp* package in R [12]. We test both models with one, two and three segments between two intercepts to cover possible changes in the speed of decrease of  $R_0$  between assuming stable baseline and final post-NPI states as observed in exploratory analysis. We used Bayesian leave-one-out cross-validation to select the number of changepoints [21].



SM Figure 9: Cantonal-level probability that  $R_0$  was below one at dates of NPIs. National scale probability denoted by 'CH'. NPI numbers correspond to 1) Ban of events of more than 1000 people on February 28, 2) School closure on March 13, 3) Closure of all non-essential commercial activities on March 16, 4) Ban of gatherings of more than 5 people and recommended home isolation on March 20.



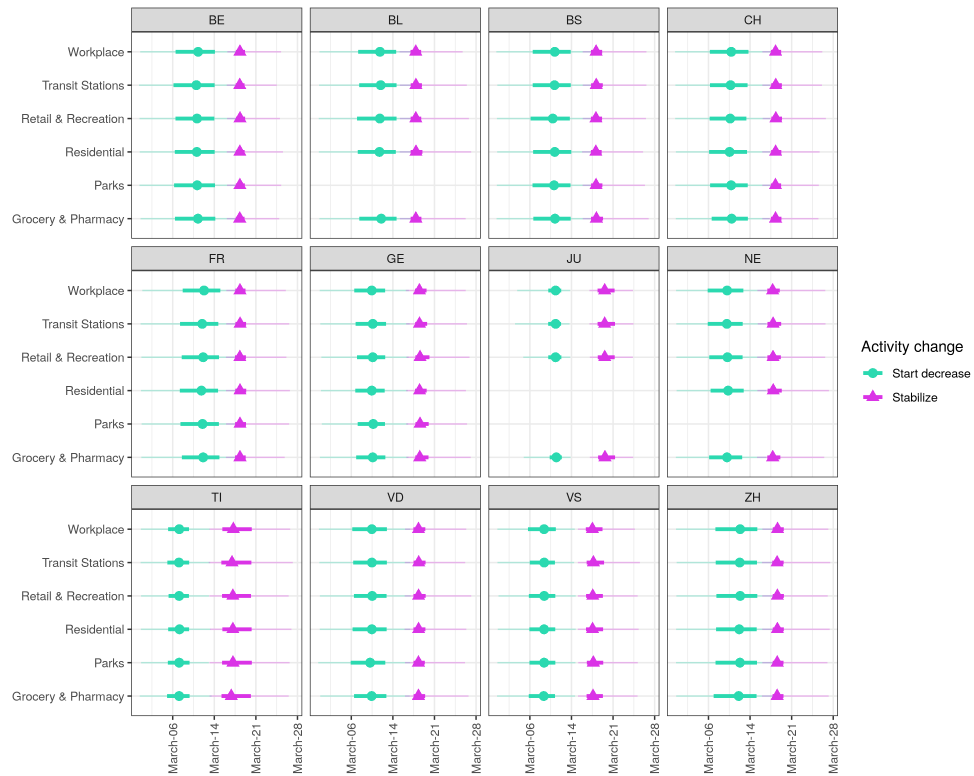
SM Figure 10: Date at which  $R_0$  fell below 1. Estimates are shown in terms of the median (point), IQR (thick error bars) and 95% quantile range (error bars). National crossing date denoted by 'CH'.



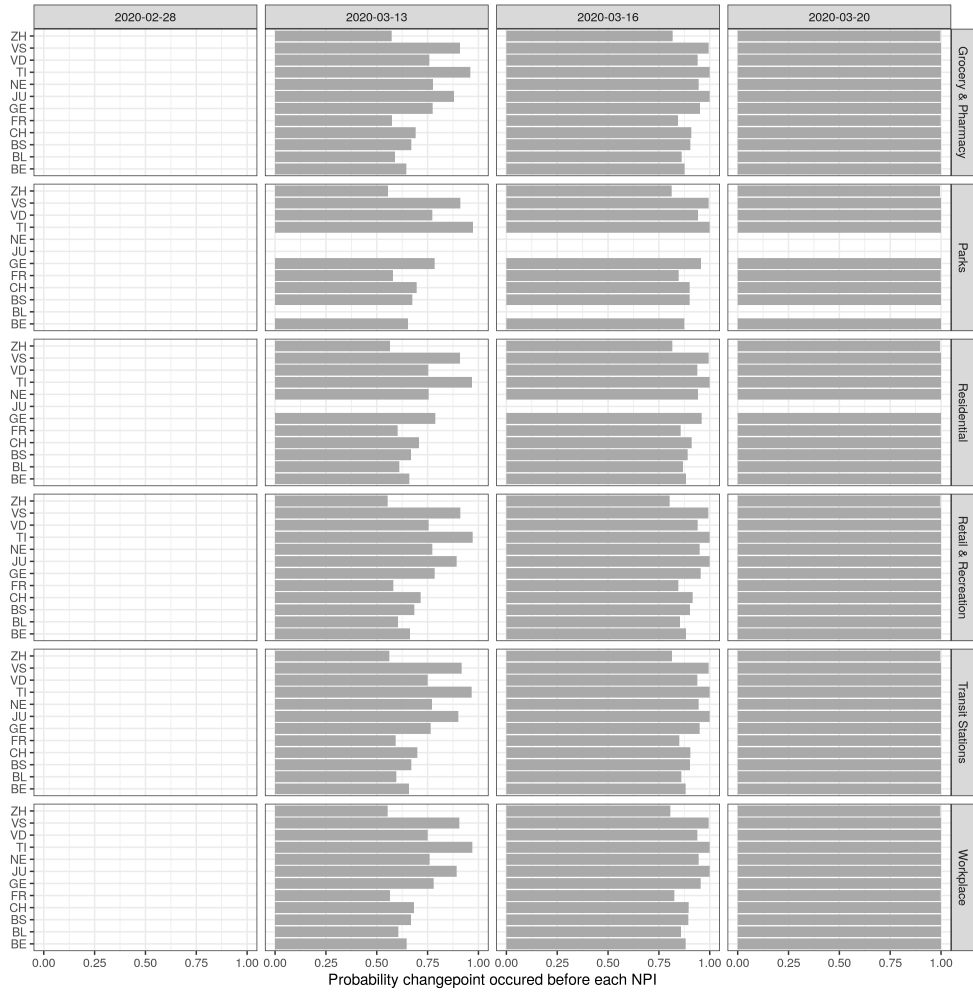
SM Figure 11: Changepoints of  $R_0$  and dates of NPIs. Left: Dates of initiation and stabilization of reduction in  $R_0$  based on changepoint models with single slope in terms of the median (points), IQRs (thick error bars) and 95% quantile ranges (error bars). Right: Posterior probabilities that  $R_0$  started decreasing before the date of implementation of NPIs as described in Figure 1 of the main text. National-level estimates are denoted by 'CH'.

SM Table 7: Model comparison results of changepoint models applied to estimated  $R_0$  time series. We considered models with two plateaus connected by either one (model1), two (model2) or three (model3) distinct slopes. Model comparison was performed by Bayesian leave-one-out cross-validation [21]. Difference in estimated log pointwise predictive density (elpd) between two models are considered significant if their absolute value is larger than 5 times their standard error (SE). The best fitting model is ordered first for each canton. National scale models denoted by 'CH'.

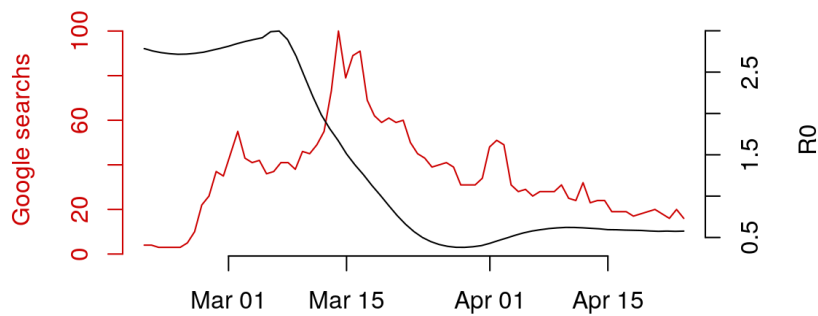
Canton	Model	LOO difference	SE	significant
BE	model3	0.00	0.00	
BE	model2	-1.80	1.35	FALSE
BE	model1	-35.07	6.60	TRUE
BL	model3	0.00	0.00	
BL	model2	-0.74	0.40	FALSE
BL	model1	-5.01	3.16	FALSE
BS	model3	0.00	0.00	
BS	model2	-35.92	5.27	TRUE
BS	model1	-36.50	5.42	TRUE
CH	model3	0.00	0.00	
CH	model2	-9.87	6.12	FALSE
CH	model1	-13.87	4.33	FALSE
FR	model3	0.00	0.00	
FR	model1	-27.41	6.71	FALSE
FR	model2	-28.32	7.33	FALSE
GE	model3	0.00	0.00	
GE	model2	-1.01	1.00	FALSE
GE	model1	-1.04	2.36	FALSE
GR	model3	0.00	0.00	
GR	model2	-9.36	3.23	FALSE
GR	model1	-12.59	4.04	FALSE
JU	model2	0.00	0.00	
JU	model1	-24.04	7.59	FALSE
JU	model3	-24.45	7.88	FALSE
NE	model3	0.00	0.00	
NE	model2	-0.01	0.27	FALSE
NE	model1	-17.39	7.16	FALSE
TI	model3	0.00	0.00	
TI	model2	-0.43	0.41	FALSE
TI	model1	-13.17	5.14	FALSE
VD	model3	0.00	0.00	
VD	model2	-15.38	5.63	FALSE
VD	model1	-45.58	5.28	TRUE
VS	model3	0.00	0.00	
VS	model2	-1.01	0.36	FALSE
VS	model1	-24.92	6.44	FALSE
ZH	model3	0.00	0.00	
ZH	model2	-5.26	6.34	FALSE
ZH	model1	-31.64	8.77	FALSE



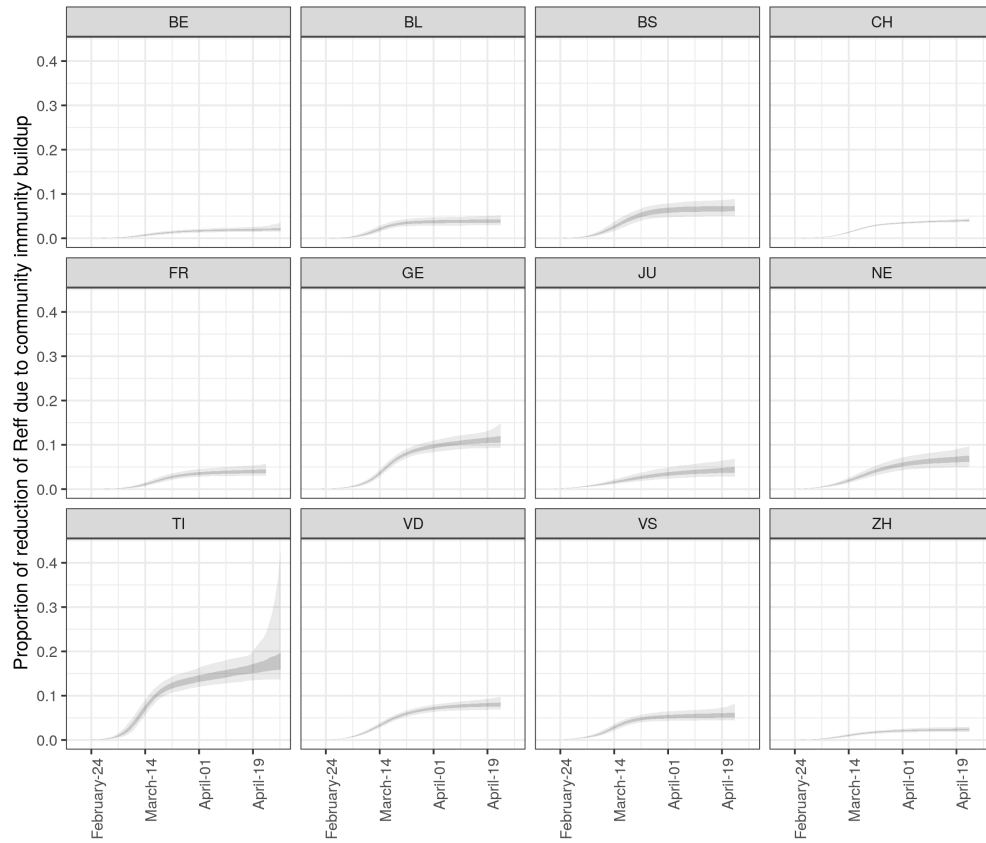
SM Figure 12: Changpoints in activity-related mobility. Dates of initiation and stabilization of reduction in each type of mobility based on changepoint models with single slope in terms of the mean (points), 50 % (thick error bars) and 95% CrI (error bars). National-level estimates are in panel 'CH'.



SM Figure 13: Posterior probabilities that activity-related mobility started decreasing before the date of implementation of NPIs as described in Figure 1 of the main text. National-level estimates are denoted by 'CH'.



SM Figure 14: Google trends for COVID-19 and changes in  $R_0$  in Switzerland. Trends corresponds to amount of searches for the keyword "coronavirus" (red line) between February 15 and April 30 and are given as a percent of the maximum number of searches in the period, time evolution of  $R_0$  from the main text.



SM Figure 15: Proportion the reduction in the effective reproduction number  $R_{eff}$  linked to depletion of susceptibles due to buildup of community immunity (through infection-derived immunity).

## References

- [1] Alexis Bellot and Mihaela Schaar. “Tree-based Bayesian Mixture Model for Competing Risks”. In: *International Conference on Artificial Intelligence and Statistics*. International Conference on Artificial Intelligence and Statistics. ISSN: 1938-7228 Section: Machine Learning. Mar. 31, 2018, pp. 910–918. URL: <http://proceedings.mlr.press/v84/bellot18a.html> (visited on 05/14/2020).
- [2] Qifang Bi et al. “Epidemiology and transmission of COVID-19 in 391 cases and 1286 of their close contacts in Shenzhen, China: a retrospective cohort study”. In: *The Lancet Infectious Diseases* (Apr. 27, 2020). ISSN: 1473-3099. DOI: 10.1016/S1473-3099(20)30287-5. URL: <http://www.sciencedirect.com/science/article/pii/S1473309920302875> (visited on 04/30/2020).
- [3] Carles Bretó et al. “Time series analysis via mechanistic models”. In: *The Annals of Applied Statistics* 3.1 (Mar. 2009), pp. 319–348. ISSN: 1932-6157, 1941-7330. DOI: 10.1214/08-A0AS201. URL: <https://projecteuclid.org/euclid.aoas/1239888373> (visited on 06/27/2019).
- [4] Bob Carpenter et al. “Stan: A Probabilistic Programming Language”. In: *Journal of Statistical Software* 76.1 (Jan. 11, 2017). Number: 1, pp. 1–32. ISSN: 1548-7660. DOI: 10.18637/jss.v076.i01. URL: <https://www.jstatsoft.org/index.php/jss/article/view/v076i01> (visited on 05/02/2020).
- [5] Tapiwa Ganyani et al. “Estimating the generation interval for COVID-19 based on symptom onset data”. In: *medRxiv* (Mar. 8, 2020). Publisher: Cold Spring Harbor Laboratory Press, p. 2020.03.05.20031815. ISSN: 10.1101/2020.03.05.20031815. DOI: 10.1101/2020.03.05.20031815. URL: <https://www.medrxiv.org/content/10.1101/2020.03.05.20031815v1> (visited on 04/25/2020).
- [6] A. C. Ghani et al. “Methods for Estimating the Case Fatality Ratio for a Novel, Emerging Infectious Disease”. In: *American Journal of Epidemiology* 162.5 (Sept. 1, 2005). Publisher: Oxford Academic, pp. 479–486. ISSN: 0002-9262. DOI: 10.1093/aje/kwi230. URL: <https://academic.oup.com/aje/article/162/5/479/82647> (visited on 05/14/2020).
- [7] Xi He et al. “Temporal dynamics in viral shedding and transmissibility of COVID-19”. In: *Nature Medicine* (Apr. 15, 2020). Publisher: Nature Publishing Group, pp. 1–4. ISSN: 1546-170X. DOI: 10.1038/s41591-020-0869-5. URL: <https://www.nature.com/articles/s41591-020-0869-5> (visited on 04/25/2020).
- [8] Angkana T. Huang et al. “A systematic review of antibody mediated immunity to coronaviruses: antibody kinetics, correlates of protection, and association of antibody responses with severity of disease”. In: *medRxiv* (Apr. 17, 2020). Publisher: Cold Spring Harbor Laboratory Press, p. 2020.04.14.20065771. DOI: 10.1101/2020.04.14.20065771. URL: <https://www.medrxiv.org/content/10.1101/2020.04.14.20065771v1> (visited on 05/15/2020).
- [9] Edward L. Ionides, C. Bretó, and Aaron A. King. “Inference for nonlinear dynamical systems”. In: *Proceedings of the National Academy of Sciences* 103.49 (Dec. 5, 2006), pp. 18438–18443. ISSN: 0027-8424, 1091-6490. DOI: 10.1073/pnas.0603181103. URL: <https://www.pnas.org/content/103/49/18438> (visited on 05/06/2019).
- [10] Aaron A. King, Dao Nguyen, and Edward L. Ionides. “Statistical Inference for Partially Observed Markov Processes via the R Package pomp”. In: *arXiv:1509.00503 [stat]* (Sept. 1, 2015). arXiv: 1509.00503. URL: <http://arxiv.org/abs/1509.00503> (visited on 05/26/2019).
- [11] Aaron A. King et al. “Inapparent infections and cholera dynamics”. In: *Nature* 454.7206 (Aug. 2008), p. 877. ISSN: 1476-4687. DOI: 10.1038/nature07084. URL: <https://www.nature.com/articles/nature07084> (visited on 12/21/2017).
- [12] Jonas Kristoffer Lindeløv. *mcp: An R Package for Regression With Multiple Change Points*. preprint. Open Science Framework, Jan. 5, 2020. DOI: 10.31219/osf.io/fzqxv. URL: <https://osf.io/fzqxv> (visited on 04/29/2020).
- [13] openZH. *openZH/covid\_19*. original-date: 2020-03-09T10:07:28Z. Apr. 25, 2020. URL: [https://github.com/openZH/covid\\_19](https://github.com/openZH/covid_19) (visited on 04/25/2020).
- [14] Daniel Probst. *daenuprobst/covid19-cases-switzerland*. original-date: 2020-03-12T12:09:53Z. May 2, 2020. URL: <https://github.com/daenuprobst/covid19-cases-switzerland> (visited on 05/02/2020).

- [15] Timothy W. Russell et al. “Estimating the infection and case fatality ratio for coronavirus disease (COVID-19) using age-adjusted data from the outbreak on the Diamond Princess cruise ship, February 2020”. In: *Eurosurveillance* 25.12 (Mar. 26, 2020). Publisher: European Centre for Disease Prevention and Control, p. 2000256. ISSN: 1560-7917. DOI: 10.2807/1560-7917.ES.2020.25.12.2000256. URL: <https://www.eurosurveillance.org/content/10.2807/1560-7917.ES.2020.25.12.2000256> (visited on 05/02/2020).
- [16] Henrik Salje et al. “Estimating the burden of SARS-CoV-2 in France”. In: *Science* (May 13, 2020). Publisher: American Association for the Advancement of Science Section: Report. ISSN: 0036-8075, 1095-9203. DOI: 10.1126/science.abc3517. URL: <https://science.sciencemag.org/content/early/2020/05/12/science.abc3517> (visited on 05/13/2020).
- [17] Jeremie Scire et al. “Reproductive number of the COVID-19 epidemic in Switzerland with a focus on the Cantons of Basel-Stadt and Basel-Landschaft”. In: *Swiss Medical Weekly* 150.1920 (May 4, 2020). Publisher: EMH Media. DOI: 10.4414/smw.2020.20271. URL: <https://smw.ch/article/doi/smw.2020.20271> (visited on 05/15/2020).
- [18] J. G. Skellam. “The frequency distribution of the difference between two Poisson variates belonging to different populations”. In: *Journal of the Royal Statistical Society. Series A (General)* 109 (Pt 3 1946), p. 296. ISSN: 0035-9238.
- [19] Office fédéral de la statistique. *Population*. Library Catalog: [www.bfs.admin.ch](http://www.bfs.admin.ch). 2018. URL: <https://www.bfs.admin.ch/bfs/fr/home/statistiken/bevoelkerung.html> (visited on 05/15/2020).
- [20] Silvia Stringhini et al. “Repeated seroprevalence of anti-SARS-CoV-2 IgG antibodies in a population-based sample from Geneva, Switzerland”. In: *medRxiv* (May 6, 2020). Publisher: Cold Spring Harbor Laboratory Press, p. 2020.05.02.20088898. DOI: 10.1101/2020.05.02.20088898. URL: <https://www.medrxiv.org/content/10.1101/2020.05.02.20088898v1> (visited on 05/14/2020).
- [21] Aki Vehtari, Andrew Gelman, and Jonah Gabry. “Practical Bayesian model evaluation using leave-one-out cross-validation and WAIC”. In: *Statistics and Computing* 27.5 (Sept. 1, 2017). Company: Springer Distributor: Springer Institution: Springer Label: Springer Number: 5 Publisher: Springer US, pp. 1413–1432. ISSN: 1573-1375. DOI: 10.1007/s11222-016-9696-4. URL: <https://link.springer.com/article/10.1007/s11222-016-9696-4> (visited on 05/01/2020).
- [22] Robert Verity et al. “Estimates of the severity of coronavirus disease 2019: a model-based analysis”. In: *The Lancet Infectious Diseases* (Mar. 30, 2020). ISSN: 1473-3099. DOI: 10.1016/S1473-3099(20)30243-7. URL: <http://www.sciencedirect.com/science/article/pii/S1473309920302437> (visited on 05/02/2020).